特集：最適化技術とその活用の最前線

3D Inverse Design Based Optimization of Axial Compressors and Turbines

L. Zhang[*1]
Advanced Design Technology, London, UK
M. Zangeneh[*1]
University College London, London, UK

1. INTRODUCTION

The aerodynamic design of gas turbine compressors and turbines has been a complex and multidisciplinary task. As part of the overall gas turbine design process, it is intertwined with aerothermodynamics and aeromechanical design. For example, the increase of turbine inlet temperature brought benefit to power output and thermal efficiency. However, the high inlet temperature requires internal cooling of the high-pressure turbine vanes and blades. The cooling flow will add to the blade passage flow and has an impact on aerodynamic performance. Meanwhile, the internal cooling flow structure also imposes geometry constraints on the three-dimensional (3D) blade shape. These all lead to additional challenges to the aerodynamic design of the blade rows. For the low-pressure stages, the high aspect ratio (span-to-chord) makes the mechanical integrity a critical issue, especially in the last stage. The design of the blade rows has to consider both aerodynamic and structural performance. Design iterations are required to satisfy both disciplines.

As the pursuit of zero emission becomes prevalent, there is an ever-growing demand on gas turbine efficiency improvement. This is the same for both stationary gas turbines and aero-engine applications. For the latter, higher rotational speed can make the structure more compact and helps to reduce the weight. However, the increased Mach number results in transonic blade flow and higher stress issue. The aerodynamic design needs to control the shock strength and the associated loss carefully.

Traditionally, the design of compressor or turbine stages started with one-dimensional (1D) meanline calculation. Then some two-dimensional (2D) through flow model was used to obtain the spanwise flow variation and the corresponding blade shape. Quasi-3D blade-to-blade calculations were quite often used to design the detail of blade shape at different spanwise sections. The 2D sections are then stacked together to create a 3D blade shape which is then evaluated by 3D CFD. Then fully three-dimensional (3D) viscous simulation was carried out to optimize the blade stacking [(1),(2)]. Quite often some iterations or optimization was needed during the 2D and Quasi-3D design. Loss models or previous design database were used during this process. Geometry scaling was also applied when developing machines of different capacities etc. Incremental changes were made to the previous existing designs [(3)]. In order to achieve a certain spanwise work distribution a number of iterations between profile sections and CFD would be required. However, this process generally relies on a large database of 2D profiles obtained from similar cases from past designs. However, with the needs to rapidly retrofit and develop gas turbines for less emission, the designers face challenges in new design space, where previous design database or guidelines may not have covered.

In the 3D inverse design approach, the blade is designed through aerodynamic inputs such as spanwise swirl velocity at inlet and exit of blade row and streamwise blade loading distribution. The solver calculates the 3D blade geometry as well as an accurate 3D inviscid flow prediction. Both the flow field information and the blade geometry are available once the solution is converged. The stacking is a design input and the inverse method automatically matches the target requirement in terms of spanwise work, streamwise blade loading and stacking condition. This design process enables designer to explore the design space without reliance on a large data base of previous designs.

One approach to overcome the limitations of the direct design process is to use automatic optimization. But for many high-speed applications in gas turbines, this requires a multidisciplinary approach which is computationally very expensive. So, there has been some reliance on the use of surrogate modelling by Artificial Neural Network (ANN). Examples can be found in [(4)-(6)]. Most of these methods built a database first to train ANN or generate a response surface model. Evolutionary algorithms based multi-objective optimization were then carried out to find the trade-off between different objectives. In these multidisciplinary design optimization strategies, the majority of the computational time is spent on the evaluation of the objective function,

原稿受付 2023年3月10日
＊1 University College London
Mechanical engineering department, Torrington place, London WC1E 7JE

using CFD and FEA. The accuracy of the ANN prediction and the response surface model depends on the quality of the database. The database has to be rebuilt if new design space is not covered by previous training data set. A considerable amount of computation effort and time has to be spent and this limits the number of designs parameters or design iterations can be investigated within the given time.

With the 3D inverse design method, a fast optimization workflow can be developed. Since the inverse design method can generate the blade geometry as well as predict the flow field information. The aerodynamic performance evaluation can be done using the loss factors (such as profile loss, leakage loss and endwall loss) calculated from the blade surface velocities. The centrifugal and bending stresses can be related to the blade geometry features. The inviscid inverse design solver can converge within a few seconds. This makes it possible to couple it to a multi-objective genetic algorithm optimizer. Hundreds of design candidates can be evaluated within a couple of hours on a single core CPU. High fidelity CFD and FEA analysis are only used for final verification.

When the 3D inverse design method is used in optimization through a Design of Experiments and surrogate model, there are also some particular advantages. Firstly, every design candidate generated by the inverse design method maintains well the specific work of the blade, as this is an input of the design. This helps to build accurate surrogate model with smaller design matrix. Secondly, the way the inverse design parametrizes the design space (by blade loading) can define a complex 3D blade geometry with less parameters, comparing to the methods that parameterize the camber line geometries with control points etc. This makes it efficient when used in optimization process, as it can explore a large design space with less degree of freedom. Finally, the flow field information can be used to check the design performance and rule out poor candidates.

In this paper, some examples of breakthrough gas turbine blade design by 3D inverse design method are provided. The paper is structured as below. In section 2, the 3D inverse design method is described. Both the inviscid and the viscous solver are discussed. In section 3, their applications to both compressor and turbine blade design are demonstrated. The transonic blade design is also covered. Section 4 discusses the optimization workflow based on inverse design method. A rapid multidisciplinary optimization of a high-speed low pressure turbine rotor is developed. Finally, a multi-point/ multi-objective optimization of a subsonic compressor stage is reviewed.

2. 3D INVERSE DESIGN METHOD

The inviscid inverse design method was developed from Hawthorne et al.'s [7] approach to represent the blades by a bound vortex sheet. The strength is determined by the specified distribution of circumferentially averaged swirl velocity:

$$r\overline{V_\theta} = \frac{N}{2\pi}\int_0^{2\pi/N} r \cdot V_\theta d\theta \quad (1)$$

Where N is the number of blades.

The method was later extended from 2D to 3D design of incompressible axial machine [8]. In the 1990s it was further developed to account for compressible flow application [9]. Since then, it has been used extensively in compressor and turbine design and optimization.

2.1 3D Inviscid Inverse Design Method

The 3D inviscid inverse design approach, TURBOdesign1 [10], is generally used for subsonic compressor and turbine blade design. The work coefficient is imposed by specifying the spanwise $r\overline{V_\theta}$ distribution at the leading edge and trailing edge of the blade. In TURBOdesign1 the $r\overline{V_\theta}$ is normalized by the blade mean radius (RMS of hub and shroud radius) and the rotational speed. For compressible flow the meridional derivative of $r\overline{V_\theta}$ is related to the enthalpy difference between the blade pressure surface and suction surface:

$$h^+ - h^- = \frac{2\pi}{N} W_{mbl} \frac{\partial(r\overline{V_\theta})}{\partial m} \quad (2)$$

If in the boundary layer local compressibility is ignored:

$$P^+ - P^- = \frac{2\pi}{N} \rho W_{mbl} \frac{\partial(r\overline{V_\theta})}{\partial m} \quad (3)$$

By prescribing the meridional derivative $\frac{\partial(r\overline{V_\theta})}{\partial m}$/ the pressure jump across the blade can be controlled. It can be imposed at two or more spanwise locations between hub and shroud.

Fig. 1 shows the streamwise blade loading ($\frac{\partial(r\overline{V_\theta})}{\partial m}$) parameterization. For each spanwise section 4 parameters (NC, ND, SLOPE and DRVTLE) are needed to define a blade loading curve. The curve consists of 3 segments. A linear line is used between NC and ND and parabolic curves are used to connect it to the LE and TE. At the trailing edge the value of $\frac{\partial(r\overline{V_\theta})}{\partial m}$ is always zero to satisfy Kutta condition. At the leading edge the DRVTLE value can be used to control the blade incidence. This type of parameterization can represent a complex 3D blade shape with 8 parameters minimum.

The following design inputs are generally required by the program:

- The meridional profile of hub, shroud, leading edge and trailing edge location
- The normal or tangential blade thickness distribution
- The inlet flow conditions in terms of spanwise distributions of total temperature and velocity components

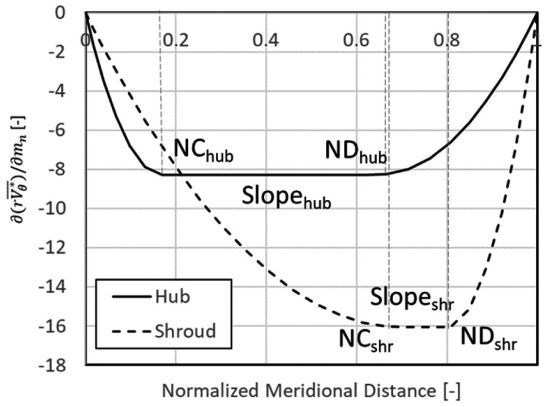

Fig. 1 The blade loading parameters used in TURBOdesign1

- The stacking condition, which can be imposed at a chord-wise station between leading and trailing edges.

The 3D blade geometry is computed by the inverse design procedure in an iterative manner. The solver converges within a few seconds and each design generated will respect the blade loading prescription. This makes it a good option as a geometry generator and a fast 3D solver, which can be coupled to optimizer in automated optimization workflow [11],[12].

2.2 3D Viscous Inverse Design Method

For transonic blade rows, shock waves play an important role in the passage flow. The presence of strong shock is associated with high loss. It also interacts with the boundary layer flow and tip clearance flow. The control of shock strength is critical for the transonic blade design. A viscous 3D inverse design method should be used to capture the shock wave and take into consideration the viscous behavior. TURBOdesign2 [13], a viscous 3D inverse design method can be used to redesign and optimize the transonic blade rows. In this method, the Euler equations of motion are solved by using a cell vertex finite volume formulation and a time-marching approach which employs a four-stage Runge-Kutta method. Viscous effects are represented by a body force, and the wall shear stress is computed by means of wall functions. The code has two modes. In the 'analysis mode', the geometry is provided and the flow field is computed, the same as with a conventional CFD analysis. In the 'design mode', the blade loading is specified. The flow field and the corresponding blade geometry is calculated in an iterative manner until the calculation converges to give the final blade geometry and the corresponding steady state flow solution. The complete description of the method is reported by Tiow and Zangeneh [14]. The methodology was extended to multiple blade rows and multistage by using a characteristic type mixing plane by Ray and Zangeneh [15]. The mixing plane model takes into account the interaction between blade rows and enables design of one stage or multiple stages.

Similar to TURBOdesign1, the meridional profile, blade thickness and stacking condition can be specified as design input. The 3D viscous inverse design method can generate the blade geometry corresponding to a specified distribution of the circumferentially averaged swirl velocity ($r\overline{V_\theta}$) or the pressure loading (pressure difference across the blade), which is prescribed along the span. It has been applied to the redesign of transonic compressor [16], fan [17],[14],[15] and turbine [14],[18].

3. EXAMPLES OF BREAKTHROUGH DESIGN BY 3D INVERSE DESIGN

In this section, some examples of gas turbine blade design by the 3D inverse design method (TURBOdesign1 and TURBOdesign2) will be discussed.

3.1 Controlled Stacking for Turbine Blades

The first example is the application of 3D inviscid inverse design method (TURBOdesign1) on HP/IP turbine nozzle blade. The work was presented by Watanabe et al. in [19]. The aim of the work was to reduce the endwall loss through the use of controlled stacking. The secondary flows are caused by passage vorticities and can be predominate near the endwalls. 3D blade design through 3D stacking has been investigated to reduce the secondary flow loss in nozzles and blades [20],[21]. However, with the traditional methods, the stacking can change the exit velocity distribution due to the 3D flow redistribution effect. The designers have to perform iterative designs of 2D airfoil in order to control the exit velocity profile. With the 3D inverse design method, the distribution of $r\overline{V_\theta}$ is specified. This determines the work distribution in the blade, the stage reaction and the twisting of the blade shape. In this way the stacking effect can be studied more efficiently, without repeating the effort of adjusting the 2D airfoils along the span.

Fig. 2 shows the comparison of nozzle blade shape. The stacking condition was specified at the position of 40% axial chord distance from the leading edge. The controlled stacking has reduced wrap angle near both endwalls, which creates a local blade lean (Fig. 2, right). It is compared to the radial stacking nozzle where the blade is stacked along the radial direction (Fig. 2, left).

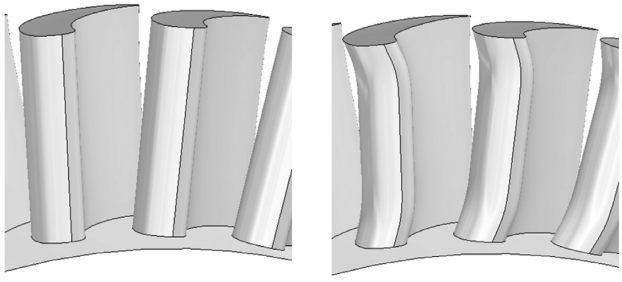

Fig. 2 Comparison of Nozzle Shape, left: radial stacking, right: controlled stacking [19].

Fig. 3 shows the CFD predicted total pressure loss coefficient at the nozzle downstream. The controlled stacking reduces the loss peaks near the endwall without increasing the losses near midspan. This is because the blade lean near the endwalls reduces the loading locally, while the midspan loading is kept almost the same as the radial stacking case. This helps to suppress the secondary flow (migrating from pressure to suction surface) near endwall, therefore the losses are reduced.

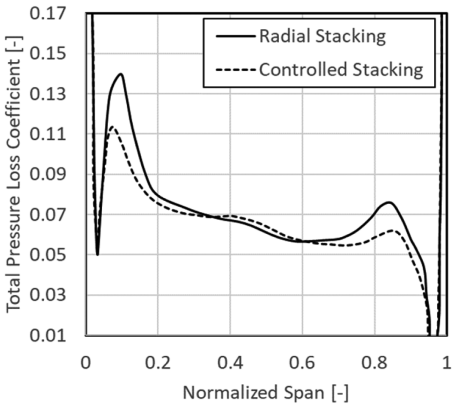

Fig. 3 Total Pressure Loss Distributions (from CFD Prediction) at Nozzle Downstream [19]

The example shows the 3D inverse design method can effectively control the secondary flow in the nozzle through the $r\overline{V_\theta}$ distribution and the controlled stacking specification. It is an efficient approach to generate 3D blade design through aerodynamics inputs.

3.2 Shock Control on Transonic Compressor Rotor

In the second example [17], the 3D viscous inverse design method (TURBOdesign2) was applied to the design of first stage rotor of Siemens SGT100 (Typhoon) compressor. The rotor has rotational speed of 17384 rpm and design point pressure ratio of 1.4. The baseline rotor has double circular arc profiles with inlet Mach number of 1.1. The Mach number contour near the tip of the baseline (conventional) rotor at peak efficiency is shown in Fig. 4. The results show a strong normal shock, with a peak Mach number of 1.44.

The corresponding loading distribution is shown in Fig. 5 for the baseline rotor as computed by TURBOdesign2. The strong jump in loading corresponds to the suction leg of the shock and clearly the results shows that the shock extends all the way to 25% span. For the redesign the blade loading was smoothed in TURBOdesign2 at 25%, 50%, 75% span and the tip while maintaining the same loading at the hub. The resulting loading distribution is shown in Fig. 6.

The resulting blade geometry near the tip and the Mach number contours are shown in Fig. 7. The blade designed by the 3D inverse design method has developed a S-shaped geometry which forms expansion waves that help to reduce

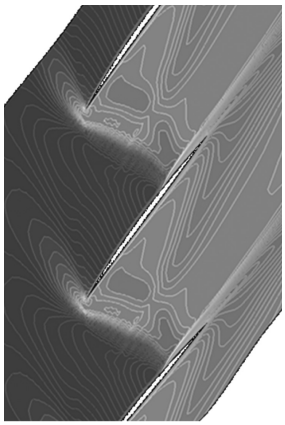

Fig. 4 Mach number distribution near the tip of baseline rotor near peak efficiency point [17]

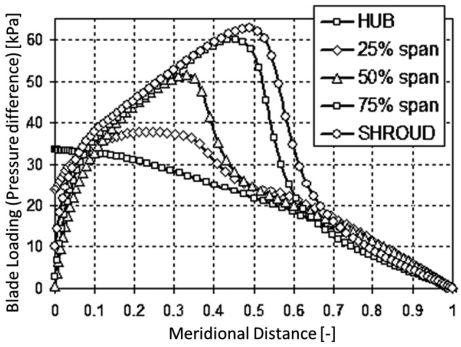

Fig. 5 The loading distribution for the baseline rotor [17]

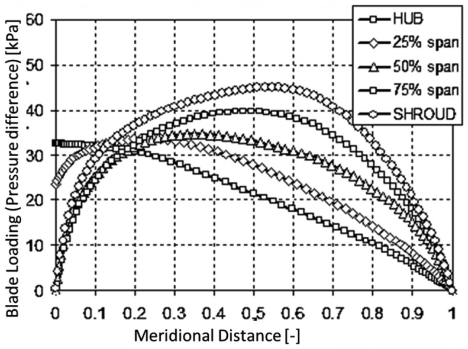

Fig. 6 The modified blade loading used in inverse design method [17]

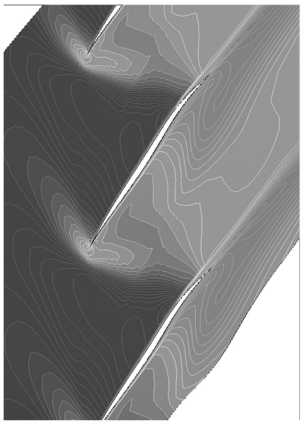

Fig. 7 Mach number distribution and geometry of inverse design rotor near the tip [17]

the shock strength. As a result, the pre-shock Mach number is reduced to 1.29 and the shock has more a bowed structure. The CFD predictions show improvement of up to 2.5 points in efficiency at design and significant improvement at off design conditions.

3.2 Shock Control on Transonic Compressor Stage

The 3D viscous inverse design method (TURBOdesign2) has also been applied to the redesign of multi-blade row transonic compressor stage in [14]. The single stage Darmstadt Transonic Compressor (DTC) (a state-of-the-art transonic compressor design representing the front stage of a high-pressure compressor in a commercial turbofan) is studied in this work. This compressor rotor (referred to as DTC Rotor 1) features high inlet relative Mach number near the rotor tip [22]. There is also strong interaction between the passage shock wave and the tip clearance flow [23]. Fig. 8 shows the computational domain of the compressor stage.

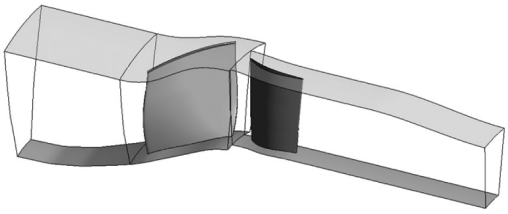

Fig. 8 DTC Rotor 1 [22]

The baseline stage rotor and stator were first analyzed in TURBOdesign2 analysis mode. The pressure loading of the rotor at peak efficiency point was then used to redesign the rotor. The stator geometry was kept unchanged but was included in the calculation to provide the correct downstream flow condition for the rotor. Tip clearance was not included in the inverse design process. But through the control of the blade loading at the shroud shock wave strength can be reduced and its interaction with the tip clearance flow can be alleviated.

Fig. 9 shows the loading distribution of the original DTC Rotor 1 (obtained from TURBOdesign2 analysis mode solution) and the loading distribution specified for the redesigned rotor at 95% span. The target loading (denoted by Target) is specified in TURBOdesign2 design mode to produce the new blade design geometry. This geometry is then analyzed in 'analysis mode' for verification. The actual loading obtained (denoted by Design) by the inverse method analysis mode is also shown on the same plot for comparison. The rapid drop in pressure loading observed for DTC Rotor1 is due to the suction surface leg of the shock wave. The redesign smoothed the shock induced loading jump in order to reduce the pre-shock Mach.

Fig. 10 the CFD predicted pressure distribution and the streamlines on the rotor suction surface. Near the shroud

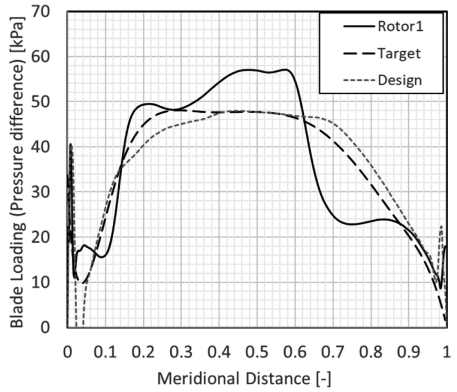

Fig. 9 Comparison of the blade loading (static pressure jump) at 95% span for original DTC Rotor 1 and the redesigned rotor at design point [22]

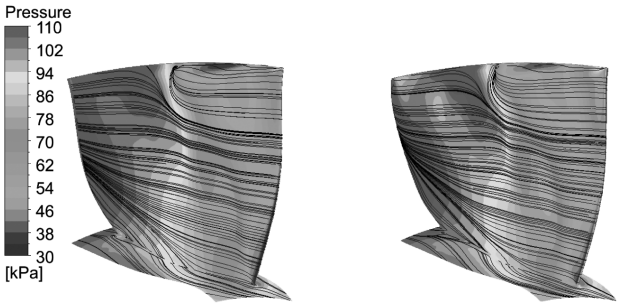

Fig. 10 Pressure distribution and streamlines on the blade suction surface at design point, left: Darmstadt transonic compressor Rotor 1; right: redesigned Rotor [22].

there is strong radial flow induced by the shock in the suction side boundary layer. For the inverse designed rotor, the low-pressure region near the tip is alleviated. This is due to the reduced shock strength and a less strong interaction between the shock wave and the tip clearance vortex.

The isentropic Mach number at 95% span is plotted in Fig. 11. It can be seen that the pre-shock Mach number is reduced for the inverse designed rotor. This shows that by smoothing the pressure loading distribution at spanwise location near the tip, the shock strength can be effectively controlled. The redesigned rotor the stage has higher total to total pressure ratio. The efficiency at 90% and 80% design rotational speed has also been improved.

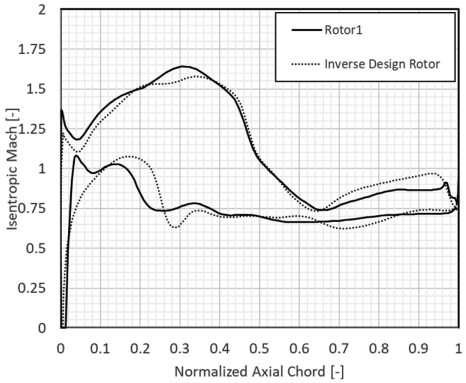

Fig. 11 Isentropic Mach Number at 95% span [22]

4. EXAMPLES OF INVERSE DESIGN BASED AUTOMATIC OPTIMIZATION

As mentioned previously, the 3D inverse design method has some advantages when coupling to an optimization algorithm. The fast solver of TURBOdesign1 makes it possible to be used in direct optimization. Instead of using time consuming CFD and FEA calculations to evaluate the objective function, both the aerodynamic performance and the blade stress can be linked to the solution of the 3D inverse design solver directly. Previous study on a pump impeller [24] compared the inverse design based direct optimization to the optimization workflow using DOE database. The results show that if the objectives and constraints are selected properly from flow physics the performance of the optimized design has very similar efficiency and suction performance compared to the optimized impeller obtained from CFD based optimization. Meanwhile, the parameterization through inverse design method was shown to be more effective in a DOE study, in comparison to the conventional way of blade parametrization which describes the camber line geometry through control points.

4.1 Rapid Multidisciplinary Optimization of LP Turbine for High-Speed Rotor

A multidisciplinary optimization was carried out for a high-speed low-pressure turbine rotor, which had been studied numerically and experimentally [5]. The LP turbine last stage rotor blade faces high stress issue as the rotational speed is increased and the number of stages reduced. The average isentropic Mach number is also increased as a result. The design optimization had to take into consideration both aerodynamic performance and mechanical concerns. Fig. 12 shows the baseline last stage stator and rotor.

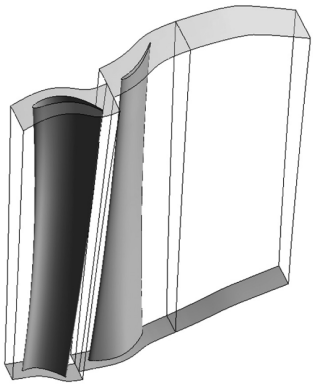

Fig. 12 Baseline Design Rotor in the Last Stage

The baseline design streamwise loading is shown in Fig. 1. The hub is evenly loaded with a zero Slopehub and the shroud is a bit aft-loaded. Zero blade incidence was assumed. Fig. 13 shows the optimization workflow. The TURBOdesign1 solver was coupled with an optimizer (TURBOdesign Optima [25]) and Multi Objective Genetic Algorithms (MOGA) was used

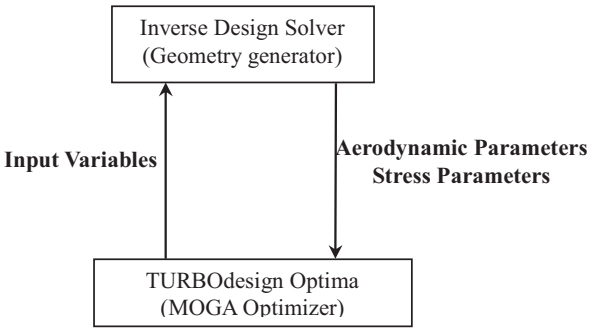

Fig. 13 Flowchart of the Direct Optimization

in the optimization.

During the optimization, the streamwise blade loading at hub, midspan and shroud was allowed to vary. The range of variation is listed in Table 1. Meanwhile, the blade thickness distribution along the span could also be adjusted. The blade thickness profile for the baseline design is shown in Fig. 14. It can be varied through a scaling factor. The scaling factor is defined at hub and shroud section. Linear interpolation is used along the span. The range of variation for scaling factors is also listed in Table 1. In total 14 parameters were allowed to vary in the direct optimization.

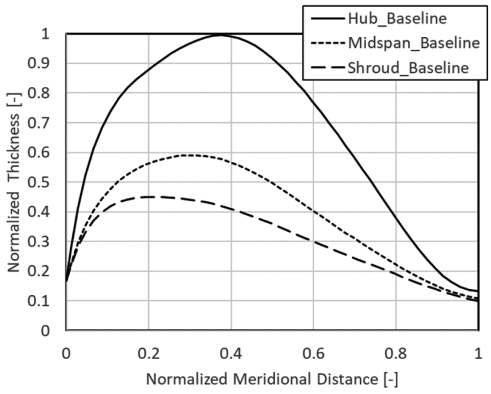

Fig. 14 Blade Thickness Profile of the Baseline Design

Table 2 shows the optimization constraints and objectives. For the aerodynamic performance, the objectives were set to minimize the blade profile loss and the endwall loss, both were calculated from the inverse design flow solution based on loss correlations [26]. For the stress control, the objectives were set to minimize the centrifugal stress and to reduce the maximum blade lean. Both could be extracted from the geometry generated by the inverse design solver. Meanwhile, the blade cross sectional area near the hub (ABladek3) was constrained to avoid increasing the hub area excessively to mitigate the stress. The diffusion ratio, maximum Mach number and throat of the rotor were also constrained. These were used to avoid flow separation, high Mach number (strong shock wave) and change of flow capacity.

Table 1 Optimization Input Variables Range

Blade Loading	
NC_{hub}	0.05 – 0.25
ND_{hub}	0.26 – 0.85
$Slope_{hub}$	-120 – 50
$DRVT_{hub}$	-6 – -2
NC_{mid}	-0.05 – 0.4
ND_{mid}	0.41 – 0.85
$Slope_{mid}$	-50 – 50
$DRVT_{mid}$	-8 – -4
NC_{shr}	-0.05 – 0.5
ND_{shr}	0.51 – 0.85
$Slope_{shr}$	-50 - 50
$DRVT_{shr}$	-6 - -2
Thickness Scaling	
ThScaleH	0.8 – 1.1
ThScaleS	0.6 – 1.1

Table 2: Optimization Constraints and Objectives

Constraints	
Throat	±1.5%
ABladek3	-11%
Diffusion Ratio	1.1 – 1.25
MaxMach	4% lower
Objectives	
ProfileLoss	Minimize
EndWallLoss	Minimize
CentrifugalStress	Minimize
MaxLean	Minimize

In total, 1600 candidates were evaluated in the direct optimization, which took several hours on a single core. Fig. 15 shows all the feasible inverse design solutions. A Pareto front was obtained between the profile loss and the endwall loss. The size of the bubbles represents the magnitude of centrifugal stress. A final 'optimized design' was selected from the Pareto front considering also the centrifugal stress and maximum lean value.

The streamwise loading distribution of the 'optimized design' is shown in Fig. 16. Compared to the baseline loading, the blade hub section is more aft-loaded. The loading at midspan and shroud is shifted upstream slightly. The incidence at the blade LE is also adjusted by the optimization. Meanwhile the optimized design decreases the blade thickness at hub and shroud. But the reduction from midspan up to the shroud is more prominent.

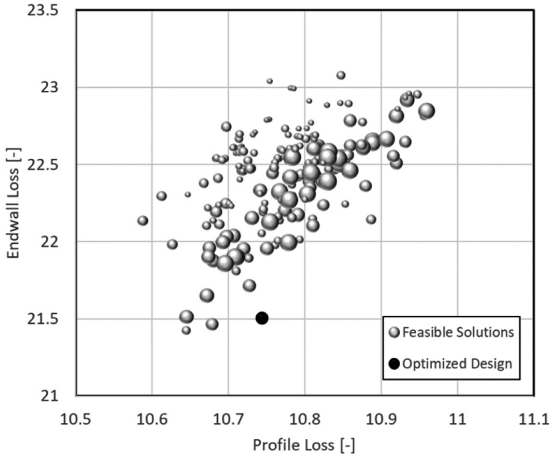

Fig. 15 Profile Loss against Endwall Loss (the Size of the Bubble Represents the Magnitude of Centrifugal Stress)

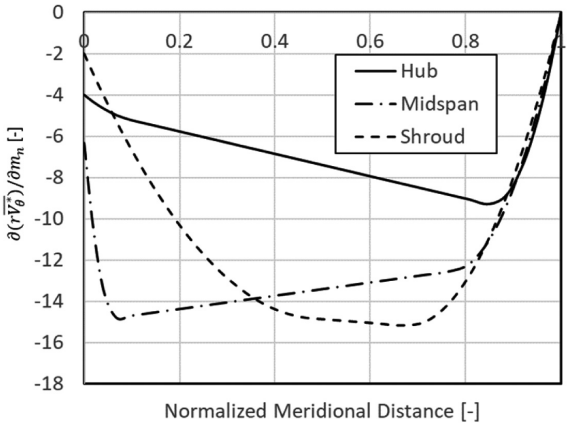

Fig. 16 Streamwise Blade Loading Distribution for the Optimized Design

The performance of the optimized rotor blade was verified through CFD simulations. Fig. 17 shows the stage efficiency is improved with the optimized rotor at various pressure ratio conditions. On the other hand, the massflow rate under different pressure ratio conditions is almost the same as the baseline design.

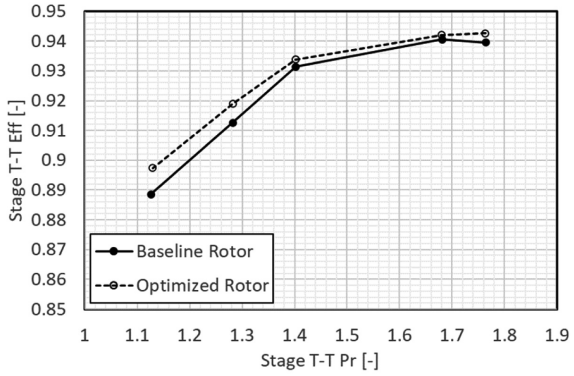

Fig. 17 Last Stage Performance with the Optimized Rotor Design

The isentropic Mach number distribution is also compared to the baseline design in Fig. 18. The optimized rotor blade reduced the maximum isentropic Mach number. This helps to reduce the transonic flow loss and improve the efficiency.

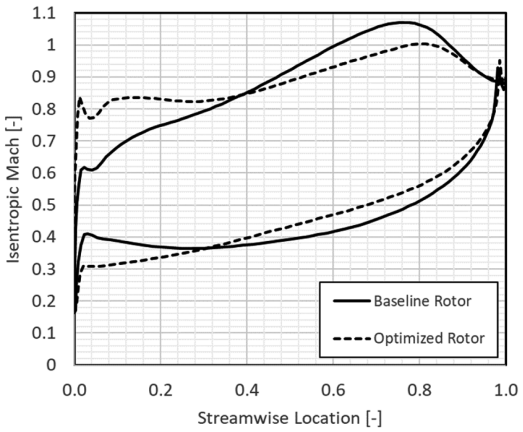

Fig. 18 Optimized Rotor Blade Surface Isentropic Mach Number at 50% span

The blade stress level of the optimized rotor was also compared to the baseline rotor blade. Fig. 19 shows the average equivalent stress along the span. The optimized design reduces the stress level along the span. The improvement in aerodynamic performance didn't lead to penalty on the blade stress level.

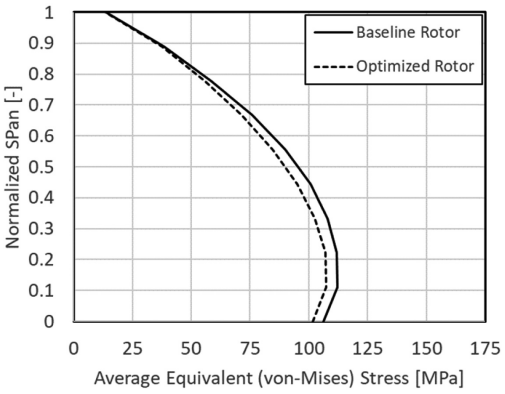

Fig. 19 Average Equivalent Stress along the Span

The example shows the direct optimization based on 3D inverse design method is efficient and effective. When the constraints and objectives are selected properly, better aerodynamic/mechanical performance can be achieved from the blade optimization. It can explore a large design space rapidly and the requirement on computational resource is low, in comparison to the optimization strategies based on CFD and FEA calculations. Furthermore, the optimum loading obtained have some generality and the experience learned can be applied to machines of different sizes. This is because the design approach uses aerodynamic inputs rather than geometrical parameters. This can help to reduce the development time for new products. The inverse design based direct optimization process generally took 4-8 hours on a single core. The time and effort spent on CFD and FEA simulation was greatly reduced. As they were needed only for the baseline and the optimized design. In contrast the CFD/FEA based optimization workflow needs hundreds of simulations to build the training dataset. It requires large computing cluster and longer computational time. The results achieved through inverse design based optimization have similar performance to the designs obtained from the conventional process [5].

4.2 Multi Point/ Multi Objective Optimization of a Subsonic Compressor Stage

In some gas turbine applications, it's important to consider performance criteria at multiple operating points. By coupling the 3D inverse design method with a surrogate model based optimization process it is quite easy to solve these multi-point/multi-objective problems in a computationally efficient manner, see [27]. In this example, the well-known HP9 compressor stage (shown in Fig. 20) consisting of rotor and stator was parametrized with 5 design parameters.

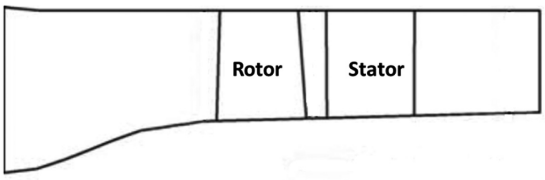

Fig. 20 The slope parameter changes for the hub and shroud and resulting loading used in optimization [27]

The location of NC and ND (as in Fig. 1) were kept fixed at 0.2 and 0.8 respectively and only the Slopehub and SlopeShr parameters were changed for the stator and rotor as shown in Fig. 21. In addition to these 4 parameters the interstage $r\overline{V_\theta}$ was also changed as shown in Fig. 22.

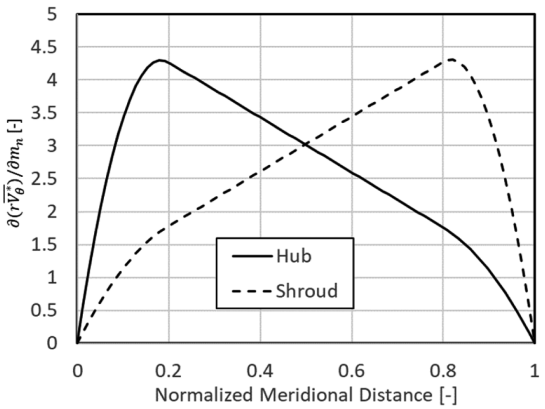

Fig. 21 The slope parameter changes for the hub and shroud and resulting loading used in optimization [27]

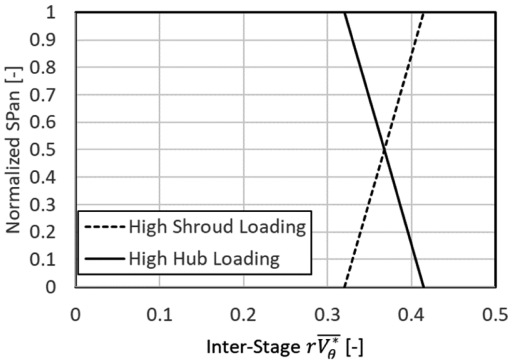

Fig. 22 Variation of interstage $r\overline{V_\theta}$ [27]

By using these five design parameters a Design of Experiment was performed to generate total of 28 stages which were then analyzed in CFD. For performance parameters the variables shown in Table 3 were used.

Table 3 Performance Parameters Used for Optimization

Variable	Operating Point
Rotor Efficiency	90%,100% and 110% Design flow
Stator loss coef.	90%,100% and 110% Design flow
Stage efficiency	90%,100% and 110% Design flow
Work Coefficient	100% design flow
Slope of the work Coefficient	
Choke Margin	

The 28 stage configurations generated by the Design of Experiment method were then run steady stage CFD to evaluate all the performance parameters shown in Table 3. Then a second order quadratic regression was used to create a surrogate model relating the performance parameters to the 5 design parameters shown in Fig. 20 and Fig. 21. Once the surrogate model was generated an optimization was run on the surrogate model using genetic algorithm looking at tradeoff between stage efficiency at 110% and 90% flow rate. Fig. 22 shows the pareto front of the optimization. An optimized solution half way on the pareto front was selected as a compromise solution between the efficiency at the two operating points. The optimized stage had fore-loaded distribution for both rotor and stator. CFD confirmed that the new stage gives higher efficiency at all operating points as compared to the baseline design.

5. CONCLUSIONS

In this paper, the application of 3D inverse design method to design of gas turbine compressor and turbine have been reviewed. Both the subsonic and transonic blade designs were discussed by using 3D inviscid and viscous inverse design

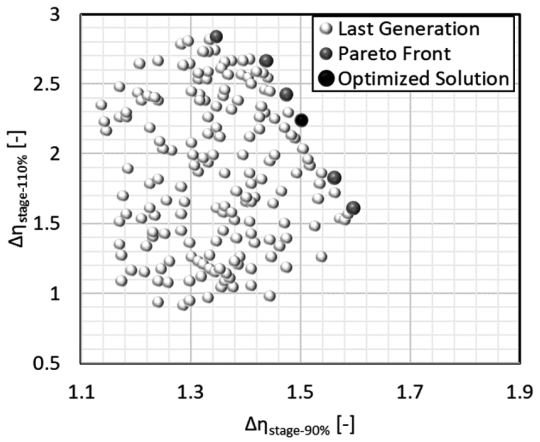

Fig. 22 Optimization Result of the axial compressor analysis [27]

methods. The key advantages of 3D inverse method in being able to handle the 3D blade design problem directly with aerodynamic parameters gives designers direct control over spanwise work distribution, streamwise loading and stacking would enable them to explore a large design space quickly without relying on database of 2D profiles and expensive CFD computations. Further it was shown that the accurate 3D inviscid solution obtained from the inviscid inverse design code in a few seconds on a single CPU core can be coupled with optimizers to rapidly look at tradeoffs in efficiency and mechanical constraints without relying on CFD or FEA. The system was applied to the design of a high speed LP Turbine for aeroengine applications.

Two examples of application of 3D viscous inverse design to transonic axial compressors were reviewed. The results show that the direct control of blade loading can help to rapidly design transonic compressor stages with controlled shock losses which is major source of loss in these types of machines.

Finally, an example of application of surrogate model based optimization, where inverse design parametrization of an axial compressor stage (rotor+stator) was used together with Design of Experiment and surrogate model based on a quadratic regression were used for rapid multi-point optimization of an axial compressor stage.

3D inverse design method can have a major impact in speeding up the process of design optimization of axial turbines and compressors used in gas turbines and aeroengines.

6. ACKNOWLEDGEMENT

This work was prepared using the info contained in (19) and we especially thank Dr. Watanabe for his support.

< REFERENCES >

(1) Denton, J. D., 2017, “Multall: An Open Source, CFD Based, Turbomachinery Design System,” ASME 2017 Turbo Expo: Turbine Technical Conference and Exposition, GT2017-63993, V02BT41A027, 14 pages, June 26-30, 2017, Charlotte, North Carolina, USA.

(2) Benini, E., 2010, “Gas Turbines: Advances in Aerodynamic Design of Gas Turbines Compressors,” Injeti, G., Sciyo, DOI: 10.5772/10205.

(3) Brandt, D. E., Wesorick, R. R., “GE Gas Turbine Design Philosophy,” GE Gas Power, GER-3434.

(4) Verstraete, T., Alsalihi, Z., Van den Braembussche, R. A., 2010, “Multidisciplinary Optimization of a Radial Compressor for Microgas Turbine Applications,” Journal of Turbomachinery, Volume 132, Issue 3, July 2010.

(5) Giovannini, M., Rubechini, F., Marconcini, M., Arnone, A., Bertini, F., 2016, “Analysis of a LPT Rotor Blade for a Geared Engine: Part I - Aero-Mechanical Design and Validation,” ASME Turbo Expo 2016: Turbomachinery Technical Conference and Exposition, GT2016-57746, V02BT38A053; 12 pages, June 13-17, 2016, Seoul, South Korea.

(6) Amedei, A., Meli, E., Rindi, A., Romani, B., Pinelli, L., Vanti, F., Arnone, A., Benvenuti, G., Fabbrini, M., Morganti, N., 2020, “Innovative Design, Structural Optimization and Additive Manufacturing of New-Generation Turbine Blades,” ASME Turbo Expo 2020: Turbomachinery Technical Conference and Exposition, GT2020-14418, V02CT35A004; 14 pages, September 21-25, 2020, Virtual, online.

(7) Hawthorne, W. R., Tan, C. S., Wang, C., McCune, J. E., 1984, “Theory of blade design for large deflections: Part I-Two-Dimensional Cascade,” J. Eng. Gas Turbines Power. Apr 1984, 106(2): 346-353 (8 pages).

(8) Tan, C. S., Hawthorne, W. R., McCune, J. E., Wang, C., 1984, “Theory of blade design for large deflections: Part II-Annular Cascades,” J. Eng. Gas Turbines Power. Apr 1984, 106(2): 354-365 (12 pages).

(9) Zangeneh, M., 1991, “A 3D Design Method for Radial and Mixed-Flow Turbomachinery Blades”, Journal of Numerical Methods in Fluids, 13, pp. 599-624.

(10) TURBOdesign1, Version 6.8.0, 2019, Advanced Design Technology Ltd. London, UK.

(11) Boselli, P., Zangeneh, M., 2011, “An Inverse Design Based Methodology for Rapid 3D Multi-Objective/Multidisciplinary Optimization of Axial Turbines,” ASME 2011 Turbo Expo: Turbine Technical Conference and Exposition, GT2011-46729, pp. 1459-1468; 10 pages, June 6-10, 2011, Vancouver, British Columbia, Canada.

(12) Zhang, L. Y., Kritioti, L., Wang, P., Zhang, J. Z., Zangeneh, M., 2022, “A Detailed Loss Analysis Methodology for Centrifugal Compressors,” J. Turbomach. May 2022, 144(5): 051013 (14 pages).

(13) TURBOdesign2, 2021, Advanced design Technology Ltd, London, UK.

(14) Tiow, W. T. and Zangeneh, M., 2000, “A Three-Dimensional Viscous Transonic Inverse Design Method,” ASME Turbo Expo, 2000-GT-0525, May 8-11, 2000, Munich, Germany.

(15) Tiow, W. T. and Zangeneh, M., 2002, “Application of a 3D viscous transonic method to NASA rotor 67,” Proceedings of the Institution of Mechanical Engineers, Part A: Journal of Power and Energy, Vol 216, 243-255.

(16) Watanabe, H. and Zangeneh, M., 2003, “Design of the Blade Geometry of Swept Transonic Fans by 3D Inverse Design,” ASME paper GT2003-38770.

(17) Bonaiuti, D., Pitigala, A., Zangeneh, M., and Li, Y., 2007, “Redesign of a Transonic Compressor Rotor by Means of a Three-Dimensional Inverse Design Method: A Parametric Study,” ASME Turbo Expo, GT2007-27486.

(18) Ray, S. R and Zangeneh, M., 2015, “A Robust Mixing Plane and Its Application in Three Dimensional Inverse Design of Transonic Turbine Stages,” Journal of Turbomachinery, Vol. 137, 011004-1-16.

(19) Watanabe, H., Harada, H., 1999, “Suppression of Secondary Flows in a Turbine Nozzle with Controlled Stacking Shape and Exit Circulation by 3D Inverse Design Method,” ASME 1999 International Gas Turbine and Aeroengine Congress and Exhibition, Paper No: 99-GT-072, V001T03A011; 12 pages, June 7-10, 1999, Indianapolis, Indiana, USA.

(20) Tanuma, T, Nagao, S, Sakamoto, T, Kawasaki, S, Matsuda, M, and Imai, K. 1995, “Aerodynamic development of advanced steam turbine blades,” Proceedings of ASME PWR, Vol.28, pp367-374, United States.

(21) Harrison, S., 1992, “The Influence of Blade Lean on Turbine Losses,” J. Turbomach. Jan 1992, 114(1): 184-190 (7 pages).

(22) Zhang, L. Y., Ray, S. R., Zangeneh, M., 2022, “Application of 3D Inverse Design Method on a Transonic Compressor Stage,” ASME Turbo Expo 2022: Turbomachinery Technical Conference and Exposition, Paper No: GT2022-82519, V10CT32A031; 14 pages, June 13-17, 2022, Rotterdam, Netherlands.

(23) Hah, C., Bergner, J., and Schiffer, H., 2006, “Short Length-Scale Rotating Stall Inception in a Transonic Axial Compressor-Criteria and Mechanisms,” ASME paper GT2006-90045.

(24) Zhang, L.Y., Davila, G., Zangeneh, M., 2021, “Multi-Objective Optimization of a High Specific Speed Centrifugal Volute Pump Using Three-Dimensional Inverse Design Coupled with Computational Fluid Dynamics Simulations,” J. Fluids Eng. Feb 2021, 143(2): 021202 (12 pages).

(25) TURBOdesign Suite, Version 6.8.0, 2019, Advanced Design Technology Ltd. London, UK.

(26) Denton, J. D., 1993, “Loss Mechanisms in Turbomachines,” the 1993 IGTI Scholar Lecture, Ohio USA, Journal of Turbomachinery 115(4), 621-656.

(27) Bonaiuti, D. and Zangeneh, M., 2009, “On the Coupling of Inverse Design and Optimization Techniques for Turbomachinery Blade Design,” J. Turbomach. Apr 2009, 131(2): 021014 (16 pages).